

# Aggregation Behavior of a Water-Soluble Terpolymer with Vinyl Biphenyl Characterized by a Fluorescent Probe

Chuanrong Zhong,<sup>1</sup> Pingya Luo,<sup>2</sup> Xianghao Meng<sup>1</sup>

<sup>1</sup>State Key Laboratory of Oil and Gas Reservoir Geology and Exploitation, Chengdu University of Technology, Chengdu 610059, Sichuan, China

<sup>2</sup>State Key Laboratory of Oil and Gas Reservoir Geology and Exploitation, Southwest Petroleum University, Chengdu 610500, Sichuan, China

Received 6 August 2008; accepted 4 July 2009

DOI 10.1002/app.31071

Published online 1 December 2009 in Wiley InterScience (www.interscience.wiley.com).

**ABSTRACT:** A terpolymer (PAAP) of acrylamide, sodium 2-acrylamido-2-methylpropane sulfonate, and vinyl biphenyl as a hydrophobic monomer was synthesized to obtain a polymeric oil-flooding agent with low molecular weight and application in oil reservoirs with medium to low permeability. The intermolecular self-assembling mechanisms in the PAAP solutions were investigated with a pyrene fluorescence probe as functions of the polymer concentration, surfactant, and temperature. The hydrophobically associating morphologies of PAAP in an unsalted solution were observed with scanning electron microscopy. The results show that the high solution viscosity of PAAP was due to the strong intermolecular hydrophobic associations of the biphenyl groups, and the critical association concentration was 0.05 g/dL for the unsalted and brine PAAP solutions. The nonpolarity and

association degree in the hydrophobic microdomains were greatly influenced by the polymer concentration. With the addition of the optimum sodium dodecyl benzene sulfonate concentration, the interpolymer hydrophobic associations were strengthened remarkably via the connection of the surfactant with biphenyl groups from different polymer chains. The number and sizes of the aggregates increased in the range of 20–50°C. These results demonstrate that the thickening effect of the PAAP polymer in the aqueous solution was due to intermolecular associations of the biphenyl groups. © 2009 Wiley Periodicals, Inc. *J Appl Polym Sci* 116: 404–412, 2010

**Key words:** association; fluorescence; microstructure; viscosity; water-soluble polymers

## INTRODUCTION

Currently, a polymer widely applied in enhanced oil recovery is partially hydrolyzed polyacrylamide (HPAM) to increase the viscosity of the aqueous phase; this results in a higher sweep efficiency. The thickening ability of HPAM relies on its superhigh molecular weight, which is generally higher than 10 million. The hydrolyzed degree is 20–30%. However, for oil reservoirs with medium to low permeabilities (permeability = 0.1–0.5  $\mu\text{m}^2$ ), HPAM is likely to plug pore throats because of the large sizes of its molecules; its high shear rate can cause the degradation of the polymer chains and result in the

irreversible decrease of the solution viscosity, and its viscosity retention ratio is only 20–30%. Hydrophobically associating acrylamide (AM)-based copolymers with a small amount of hydrophobic groups have been extensively studied.<sup>1–5</sup> Compared with HPAM, the molecular weights of these polymers are low, and above the critical association concentration ( $C_p^*$ ) in aqueous solution, the polymer molecules aggregate with each other to form large amounts of reversible supermolecular structures via the intermolecular association of hydrophobic groups; this results in a distinct increase in apparent viscosity.  $C_p^*$  is the characteristic concentration that distinguishes the dilute solution from the semiconcentrated solution. Below  $C_p^*$ , few aggregates are formed, and the apparent viscosities of the polymer solutions vary slightly.<sup>6,7</sup> Upon shearing, the associating structures are disrupted, and the degradation of polymers does not occur. However, upon removal of shear, the associations can reform, which results in the absolute recovery of the polymer solution viscosities. In addition, the polymers exhibit salt-thickening behavior.<sup>8</sup> For hydrophobically associating polymers, these unique solution properties

Correspondence to: C. Zhong (zhchrong2006@yahoo.com.cn).

Contract grant sponsor: Open Foundation of State Key Laboratory of Oil and Gas Reservoir Geology and Exploitation; contract grant number: PLC200601.

Contract grant sponsor: Postdoctoral Science Foundation of China; contract grant number: 20060391033.

prevent the inconsistency between low molecular weight and high solution viscosity and are exactly accordant with the expected molecular structure and properties of polymeric oil-displacing agents applied in oil reservoirs with medium to low permeabilities. However, the technical applications of hydrophobically modified water-soluble polymers have been still restricted as many problems have not yet been solved. For example,  $C_p^*$  is on the high side in aqueous solutions, and the viscosity below  $C_p^*$  is not high enough to be applied in enhanced oil recovery because the molecular weight is too low. In addition, most hydrophobic monomers, including derivatives of AM, acrylic esters, and their derivatives,<sup>9–12</sup> easily hydrolyze under acidic or basic conditions at high temperatures; this results in an abrupt decrease in the polymer solution viscosities. The associating behavior in aqueous solutions were investigated with a pyrene fluorescence probe for numerous associative copolymers,<sup>13–16</sup> and these articles mainly discussed the influence of some factors on the hydrophobic associations, such as the aforementioned monomer types, the block nature of the molecular backbones, the polymer concentration, and the pH values. Moreover, the solution viscosities of associative polymer/surfactant systems have also been largely studied.<sup>17–20</sup> However, the influence of the surfactant concentration and temperature on associative microstructures has not been reported in the literature.

To obtain a polymeric oil-displacing agent with good solution properties, such as high viscosity, salt thickening, shear resistance, aging resistance, and sizes of molecular chains that could match those of pores in oil reservoirs with medium to low permeability, in this study, we synthesized a novel hydrophobically associating AM-based terpolymer P(AM-NaAMPS-VP) (PAAP) with sodium 2-acrylamido-2-methylpropane sulfonate (NaAMPS) and vinyl biphenyl (VP) as a hydrophobic monomer by micellar polymerization. The biphenyl groups linked directly with the polymer main chains were stable at high temperatures. The groups from VP could induce van der Waals interactions because of its plane and polarizable structure and could greatly improve the rigidity of the polymer main chains as pendant side chains. In this study, we aimed to examine the intermolecular hydrophobic association of PAAP in unsalted and brine solutions by means of fluorescent probe measurements and to explore the variation of a hydrophobic microenvironment with parameters such as polymer concentration, surfactant concentration, and temperature. In addition, the polymer solution viscosities were measured to reveal the relationship between the thickening properties and the microstructures of the PAAP polymer in aqueous solution.

## EXPERIMENTAL

### Reagents

AM was recrystallized twice from  $\text{CHCl}_3$ , VP was obtained from Acros Organics Co. (Beijing, China), and 2-acrylamido-2-methylpropane sulfonate (AMPS) was purchased from Lubrizol Co. Other reagents were analytically pure and were used without further purification.

### Elemental analysis

The carbon, nitrogen, and hydrogen contents of the polymers were determined with a CARLO ERBA-1106 elemental analyzer (Milan, Italy), and according to the measured elemental composition data, the molar percentage compositions of the polymers were calculated.

### Ultraviolet (UV) spectral analysis

The UV spectrum was obtained with a UV-240 spectrophotometer (Shimadzu Co., Kyoto, Japan). The purified PAAP polymer was dissolved in pure water, and the polymer concentration was 0.1 g/dL.

### Fourier transform infrared (FTIR)

The FTIR spectrum was conducted with a Nicolet 560 FTIR spectrophotometer (Madison, WI) with a resolution capacity of  $1 \text{ cm}^{-1}$  and a scanning number of 32. The KBr pellet was prepared with the purified polymer sample.

### $^1\text{H-NMR}$

The purified PAAP copolymer solution in  $\text{D}_2\text{O}$  was measured at room temperature with an Inova 400-MHz instrument (Varian Co., USA) to determine whether the VP hydrophobic units were incorporated into the polymer molecules.

### Fluorescence spectroscopy

Fluorescence spectra were recorded on a Hitachi 850 spectrofluorometer (Tokyo, Japan) at  $35^\circ\text{C}$ . Pyrene was used as a micropolarity-sensitive probe, whose concentration in the polymer solutions was  $3 \times 10^{-5} \text{ mol/L}$ . The excitation wavelength was 333 nm, and the emission spectra were recorded between 350 and 600 nm with slit widths of 2 nm (excitation) and 3.0 nm (emission) at a scanning speed of 60 nm/min. We prepared polymer aqueous solutions of 0.03–0.5 g/dL by allowing the polymer to dissolve in the distilled water.

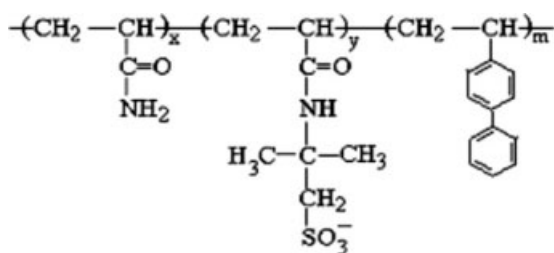


**Figure 1** Schematic representation of the molecular structure of PAAP.

### Scanning electron microscopy (SEM)

The SEM images were made with an S-3000N scanning electron microscope (Hitachi). The polymer solution sample was covered on a round plate and dried naturally to form a layer of film. Gold was sputtered on the film for electric conduction.

### Apparent and intrinsic viscosity measurements

Polymer solutions were prepared by dissolution of the purified polymer in the distilled water or NaCl aqueous solution. The apparent viscosities of the polymer solutions were measured with a Brookfield DVIII R27112E viscometer (USA) at a shear rate of  $7.34 \text{ s}^{-1}$  at  $25^\circ\text{C}$ . The intrinsic viscosities were measured by a 0.6-mm Ubbelohde capillary viscometer at  $(30.0 \pm 0.1)^\circ\text{C}$ , and 1 mol/L sodium nitrate was used as a solvent.

### Synthesis of the copolymers

The PAAP terpolymer was prepared by free-radical micellar copolymerization.<sup>21,22</sup> A 100-mL, three-necked round flask was equipped with a mechanical stirrer, a nitrogen inlet, and an outlet. AM (5.0 g, 0.0704 mol, 90.2 mol %), AMPS (1.4558 g, 0.007024 mol, 9 mol %), and sodium dodecyl sulfate (SDS; 1.1166 g) were dissolved in 29.94 mL of distilled water, and the solution was placed in the flask. NaOH was used to control the pH value of the reaction solution between 6 and 7. The mixture was stirred for 15 min, and VP ( $0.1124 \text{ g}, 6.2430 \times 10^{-4} \text{ mol}, 0.8 \text{ mol } \%$ ) was then added to the reaction flask. The flask was purged with  $\text{N}_2$  for 0.5 h. The reactant solution was heated to  $50^\circ\text{C}$  with stirring in a tempering kettle under a nitrogen atmosphere, and 7.28 mL of a 0.005-mol/L  $\text{K}_2\text{S}_2\text{O}_8$  solution was then added to the reactant solution. After the polymerization proceeded for 16 h at  $50^\circ\text{C}$ , the reaction mixture was diluted with 500 mL of distilled water, and two volumes of acetone were then added with stirring to precipitate the polymers. The polymers were washed with acetone twice and extracted with ethanol by the Soxhlet extraction instrument for 2 days to

**TABLE I**  
FTIR Vibration Peaks of the PAAP Polymer

Group	Vibration type	Wave number ( $\text{cm}^{-1}$ )
—N—H	Stretching	3417.44
C=O	Stretching	1663.07
—CH <sub>3</sub> , —CH <sub>2</sub> , —CH	Stretching	2851.63, 2933.18, 2785.19
—CH <sub>3</sub> , —CH <sub>2</sub> , —CH	Bending	1452.05, 1415.24, 1349.65
=C—H in biphenyl	Stretching	3200.00
=C—H in biphenyl	Bending	762.00
—SO <sub>3</sub> <sup>−</sup>	Bending	1187.92, 1119.59, 1040.61

remove all traces of water, surfactant, residual monomers, and initiator. Finally, the polymers were dried under vacuo at  $50^\circ\text{C}$  for 3 days.

In the absence of the hydrophobic monomer VP, P(AM-NaAMPS) (PAA) was synthesized, and the reaction conditions and purification method were the same as those mentioned earlier.

The molecular structure of PAAP is shown in Figure 1. The intrinsic viscosities of PAA and PAAP were 10.27 and 4.83 dL/g, respectively, and the molar composition of the two polymers were AM/NaAMPS = 88.49 : 11.51 and AM/NaAMPS/VP = 88.21 : 10.83 : 0.96, respectively. For the UV spectrum of PAAP, there was a typical absorption peak at 240 nm attributed to the aromatic multiring structure. The FTIR peaks and  $^1\text{H-NMR}$  (400-MHz) shifts of PAAP are shown in Tables I and II, respectively.

## RESULTS AND DISCUSSION

### Unsalted and brine PAAP solutions

The fluorescent probe technique is used to investigate the formation of the microenvironment, and the probe is commonly pyrene, the solubility of which in water is very low (ca.  $1.0 \times 10^{-7} \text{ mol/L}$ ). However, pyrene is preferably solubilized in hydrophobic microdomains. Among various fluorescent probes, the vibrational fine structure of the emission

**TABLE II**  
 $^1\text{H-NMR}$  Shifts ( $\delta$ ) of the PAAP Polymer

Group	$\delta$ (ppm)
9H (—CH of biphenyl)	7.377–7.823
2H (—CH <sub>2</sub> of the VP main chain)	3.441
1H (—CH of the VP main chain)	3.210
6H (—CH <sub>3</sub> of the NaAMPS side chain)	1.497
2H (—CH <sub>2</sub> of the AMPS side chain)	3.665
2H (—CH <sub>2</sub> of the NaAMPS main chain)	1.787
1H (—CH of the AMPS main chain)	2.357
2H (—CH <sub>2</sub> of the AM main chain)	1.673
1H (—CH of the AM main chain)	2.228

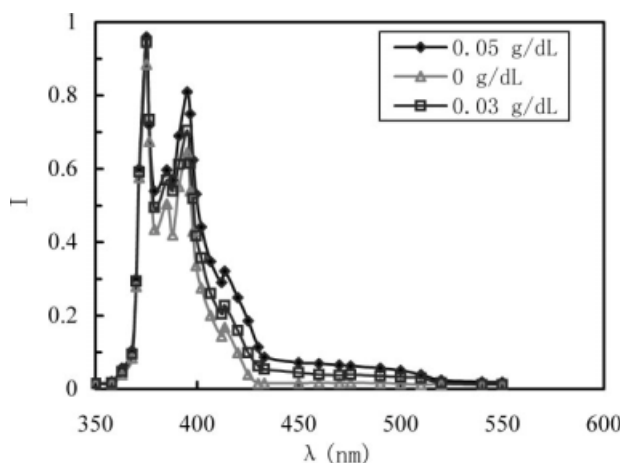


**Figure 2** Fluorescence spectra of pyrene in dilute unsalted solutions with different PAAP concentrations ( $\lambda$  = wavelength;  $I$  = intensity).

spectrum of pyrene is the most sensitive to the change in located microenvironment.<sup>23–26</sup> The intensity ratio of the first vibronic peak at 375 nm to the third vibronic peak at 384 nm ( $I_1/I_3$ ) in the fluorescence emission spectrum is sensitive to the polarity of the hydrophobic microenvironment in which the pyrene probe is located. Thus, the formation of hydrophobic microdomains in aqueous solution can be shown by a decrease in the  $I_1/I_3$  value.

The pyrene emission spectra for the PAAP polymer in dilute and semiconcentrated unsalted solutions are shown in Figures 2 and 3, respectively. Figures 4 and 5 show the pyrene emission spectra of the polymer in 0.256-mol/L NaCl solutions. According to the previously shown pyrene emission spectra, the plots of  $I_1/I_3$  versus polymer concentration are displayed in Figure 6 for PAAP in unsalted and brine solutions. As shown in Figures 2 and 6, the

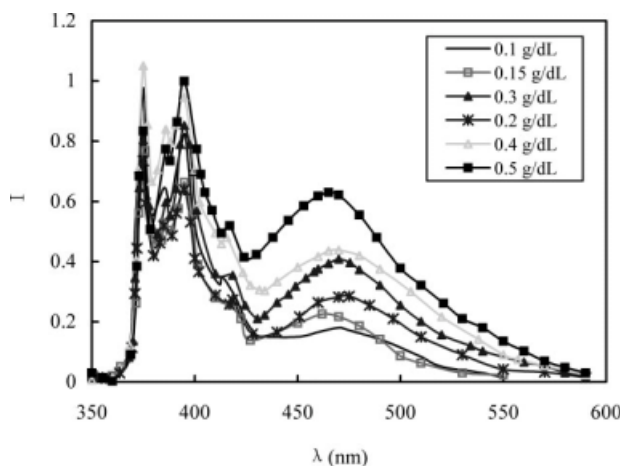


**Figure 3** Fluorescence spectra of pyrene in semiconcentrated unsalted solutions with different PAAP concentrations ( $\lambda$  = wavelength;  $I$  = intensity).

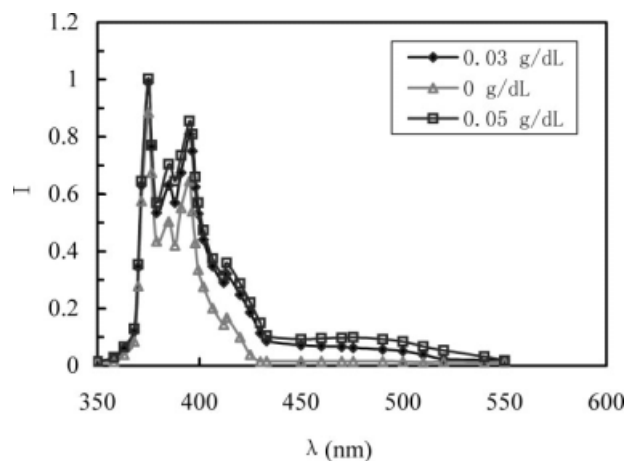


**Figure 4** Fluorescence spectra of pyrene in 0.256 mol/L NaCl dilute solutions with different PAAP concentrations ( $\lambda$  = wavelength;  $I$  = intensity).

$I_1/I_3$  values was 1.660 at a polymer concentration of 0.03 g/dL and was slightly lower than that in pure water (1.76). The result suggests that some hydrophobic microdomains were formed in the polymer solution as well as a majority of monomolecules. The  $I_1/I_3$  value dropped remarkably from 1.66 to 1.500 with increasing polymer concentration from 0.03 to 0.1 g/dL and then decreased slightly in a polymer concentration range of 0.1–0.2 g/dL. Finally, the  $I_1/I_3$  value was 1.077 at a polymer concentration of 0.5 g/dL, which indicated that the nonpolarity in hydrophobic microenvironments was almost the same as that of micelles in 0.05-mol/L SDS aqueous solution ( $I_1/I_3 = 1.05$ ).<sup>27</sup> The variation of  $I_1/I_3$  with polymer concentration revealed that the intermolecular hydrophobic associations were strengthened with increasing polymer concentration, which led to a great increase in the nonpolarity of the pyrene microenvironments. Moreover, it

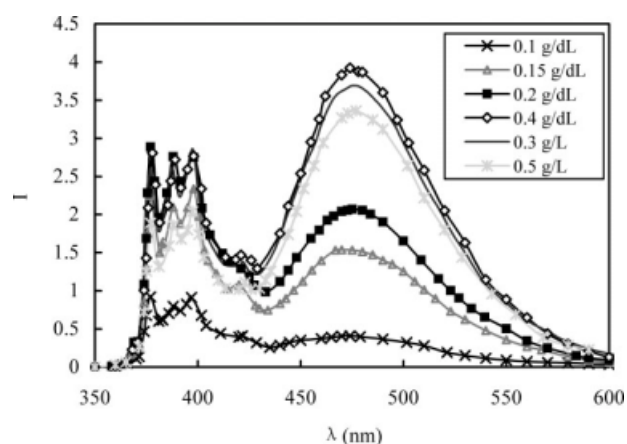


**Figure 5** Fluorescence spectra of pyrene in 0.256 mol/L NaCl semiconcentrated solutions with different PAAP concentrations ( $\lambda$  = wavelength;  $I$  = intensity).

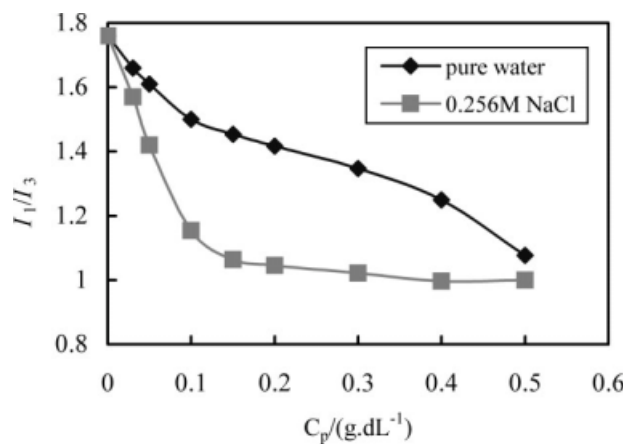


**Figure 6** Influence of the PAAP concentration ( $C_p$ ) on  $I_1/I_3$  values in unsalted and NaCl solutions.

revealed that large amounts of hydrophobic microdomains formed at 0.1-g/dL PAAP.

In a 0.256-mol/L NaCl solution, at the same polymer concentration, the  $I_1/I_3$  value in brine solution was remarkably lower than that in unsalted solution, which indicated that the hydrophobic microdomains became more compact; this led to an obvious increase in the nonpolarity of the pyrene environments. The  $I_1/I_3$  value decreased dramatically from 1.570 to 1.154 with increasing polymer concentration from 0.03 to 0.1 g/dL and then gradually dropped to 1.064 at 0.15 g/dL PAAP. Finally, the  $I_1/I_3$  value tended to be constant, and the nonpolarity was almost invariable in hydrophobic microdomains, where the intermolecular associations of hydrophobic groups were balanceable with the electrostatic repulsion of  $-\text{SO}_3^-$  groups. The results show that with addition of NaCl, intermolecular repulsion was weakened because of the electrostatic shielding of  $\text{Na}^+$  on  $-\text{SO}_3^-$  groups in the polymer chains, and hydrophobic groups arranged more closely, which resulted in a remarkable increase in the nonpolarity of hydrophobic microdomains. In Figure 6, the  $I_1/I_3$  data in unsalted and brine solutions could not obviously display the  $C_p^*$  values and merely suggested that  $C_p^*$  should be lower than 0.1 g/dL.

The fluorescence emission spectrum of the excited pyrene ( $\text{Py}^*$ ) consisted of major peaks at 375, 384, and 399 nm (monomer emission peaks with intensity  $I_m$ ) in the absence of pyrene-pyrene interactions. Excimer formation occurs when the pyrene concentration in the hydrophobic microenvironment is high enough for a  $\text{Py}^*$  and a pyrene in its ground state to come into close proximity during the  $\text{Py}^*$  lifetime. The pyrene excimer emission peak (with intensity  $I_e$ ) is characterized by a broad featureless spectral emission peak centered at 475 nm. Hence, the  $I_e/I_m$  ratio has often been used as an indicator of the degree of interaction between fluorophores.<sup>28</sup> For hydrophobically

associating polymers, the  $I_e/I_m$  ratio provides a measure for characterizing the association degree of hydrophobic segments in the polymer chains and the microviscosity of the hydrophobic microdomains.

As shown in Figures 3 and 5, the excimer emission peak became obvious above a polymer concentration of 0.05 g/dL. Figure 7 shows plots of  $I_e/I_m$  as a function of the polymer concentration in unsalted and 0.256-mol/L NaCl solutions, respectively. With increasing polymer concentration for the unsalted and brine solutions, the  $I_e/I_m$  values slightly increased below 0.05-g/dL PAAP and then increased dramatically up to a polymer concentration of 0.2 g/dL. This showed sufficiently that  $C_p^*$  was 0.05 g/dL for the solutions, and above this concentration, intermolecular hydrophobic associations increased sharply. For the unsalted solution, the  $I_e/I_m$  ratio was almost invariable in the concentration range of 0.2–0.4 g/dL, which indicated that the degree of hydrophobic associations and the concentration of pyrene excimers dissolved in hydrophobic microdomains tended to be constant, although the number and sizes of aggregates increased. Finally, the  $I_e/I_m$  value increased to 0.635 at 0.5 g/dL PAAP. However, for the 0.256-mol/L NaCl solution, the intramolecular or intermolecular associations of hydrophobic groups were much stronger than those in the unsalted solution at any polymer concentration higher than 0.03 g/dL, and the  $I_e/I_m$  value abruptly increased from 0.820 to 1.647 with increasing polymer concentration from 0.2 to 0.5 g/dL.

Figure 8 shows the apparent viscosity as a function of the polymer concentration for the unsalted PAAP solution.  $C_p^*$  was 0.05 g/dL, and with increasing polymer concentration, the apparent viscosity slowly increased below 0.05 g/dL and then increased dramatically. Compared with the unsalted PAAP solution, the PAA polymer exhibited common viscosity behavior of a polyelectrolyte, and the

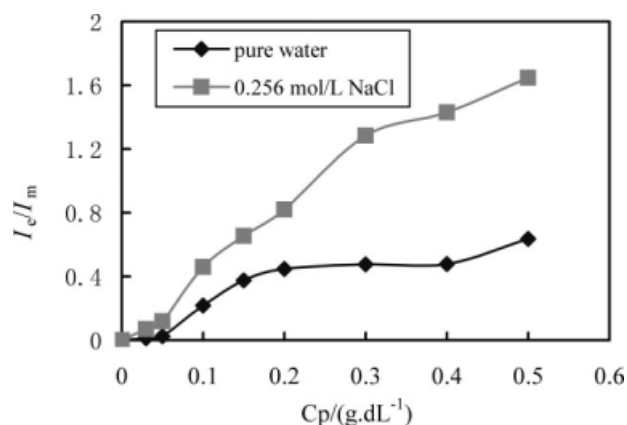


**Figure 7** Influence of the PAAP concentration ( $C_p$ ) on  $I_e/I_m$  values in unsalted and brine solutions.

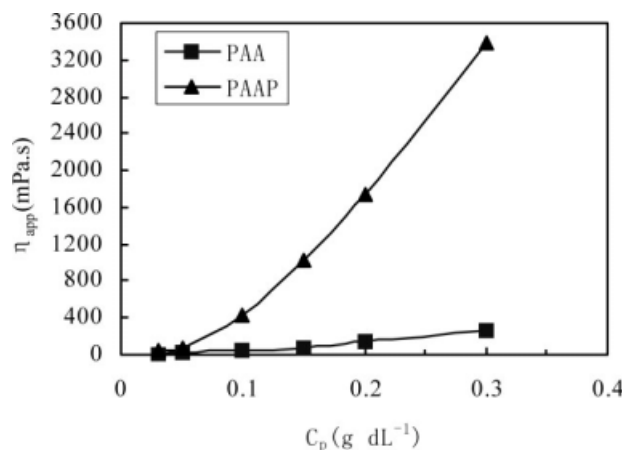


**Figure 8** Influence of the polymer concentration ( $C_p$ ) on the apparent viscosity ( $\eta_{app}$ ) of unsalted PAAP solutions.

solution viscosity linearly increased with increasing polymer concentration. The values of the apparent viscosity in Figure 8 were measured at a fixed shear rate of  $7.34 \text{ s}^{-1}$ , and the variation of apparent viscosity with shear rate was investigated by steady-shear measurement with a Gemini 200 dynamic rheometer

(Malvern Instruments Co., England).<sup>29</sup> The previously reported studies showed that the viscosities measured at  $7.34 \text{ s}^{-1}$  were all at the shear thinning phase in three consecutive shear cycles of 0.1- and 0.15-g/dL unsalted PAAP solutions. This also indicated that intermolecular hydrophobic associations still existed in the solutions at the shear rate. The fluorescent probe results were consistent with the solution viscosity measurements. These results also show that the number of microdomains and solution viscosities abruptly increased because of the formation of the three-dimensional networks via intermolecular hydrophobic associations (Fig. 9) with increasing polymer concentration above 0.1-g/dL PAAP, although the nonpolarity of the hydrophobic microdomains gradually decreased because of the balance between the intermolecular electrostatic repulsions of  $-\text{SO}_3^-$  groups and associating interactions of hydrophobic groups. As shown in Figure 9(a,b), continuous three-dimensional network structures were formed at 0.1-g/dL PAAP, but the sizes of the network bones were small. With increasing polymer concentration from 0.1 to 0.2 g/dL, the associating network structures became

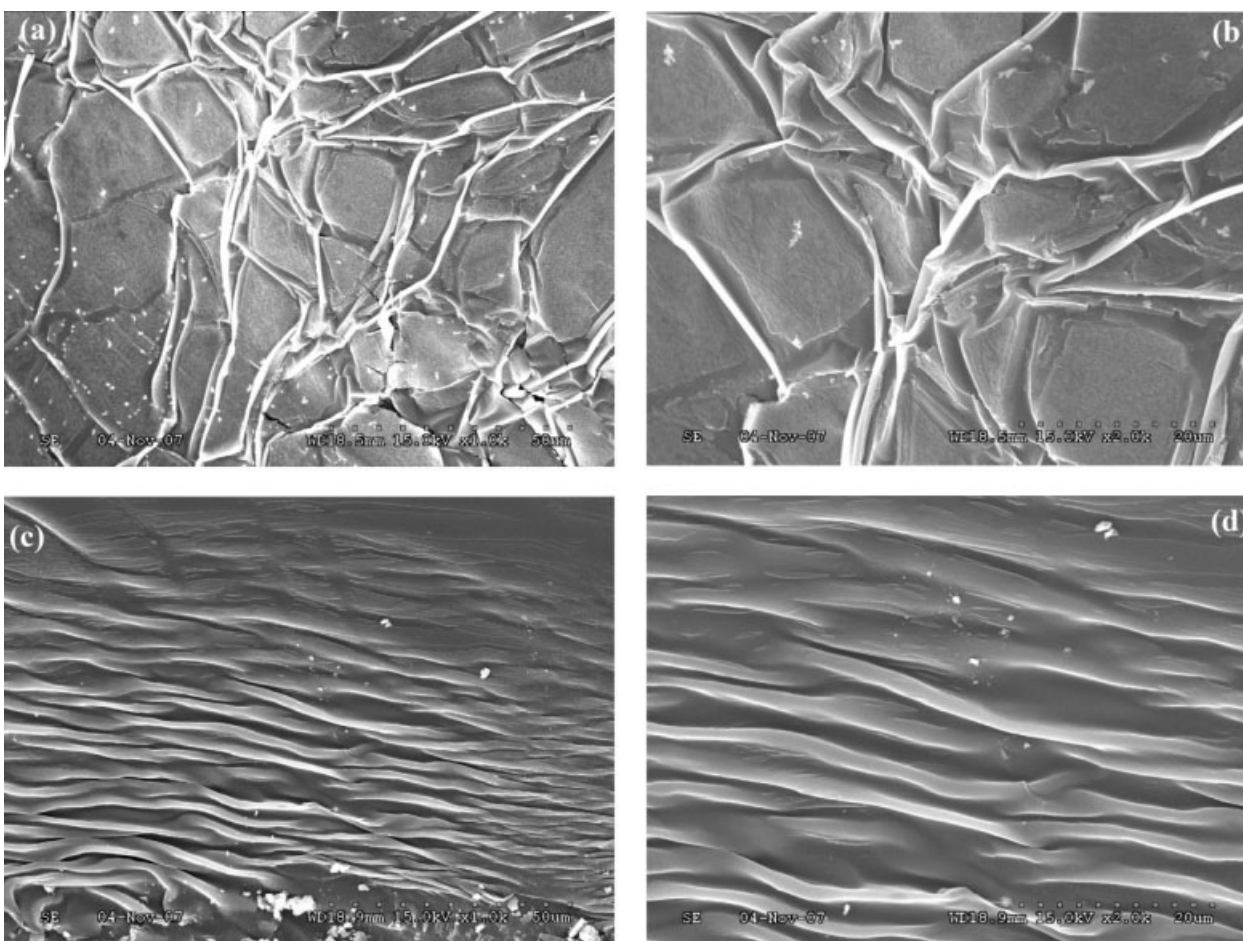


**Figure 9** SEM images of unsalted PAAP solutions: (a,b) 0.1 and (c,d) 0.2 g/dL PAAP.

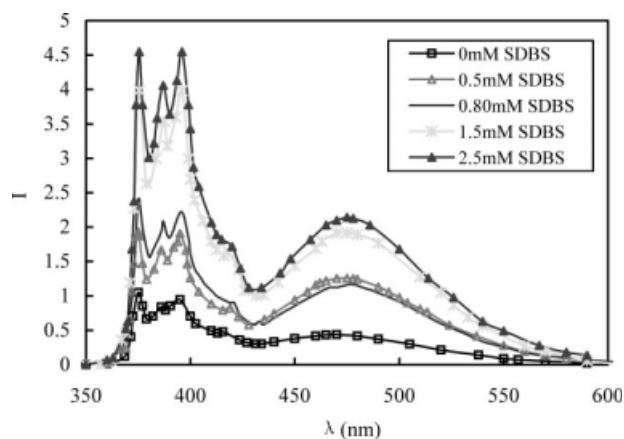


**Figure 10** Fluorescence spectra of pyrene in unsalted PAAP solutions containing SDBS ( $\lambda$  = wavelength;  $I$  = intensity). The polymer concentration was 0.4 g/dL.

much larger and compact because of more hydrophobic groups participating in intermolecular association [Fig. 9(c,d)]; this resulted in a remarkable increase in the solution viscosities. Figures 8 and 9 also show that the change in associating morphologies was in accordance with that of the solution viscosities with increasing polymer concentration, and the thickening properties of the PAAP polymer mainly depended on the associative structures.

The aforementioned results reveal that the formation of supermolecular aggregating structures resulted in a high apparent viscosity because of the strong hydrophobic associations of biphenyl groups for PAAP in pure water. In the unsalted solution, the hydrophobic microdomains were loose because of the intermolecular electrostatic repulsions of  $-\text{SO}_3^-$  groups, in which the nonpolarity was not high. Therefore, the aggregates possessed large hydrodynamics volumes, which resulted in high solution viscosities. With the addition of NaCl, the

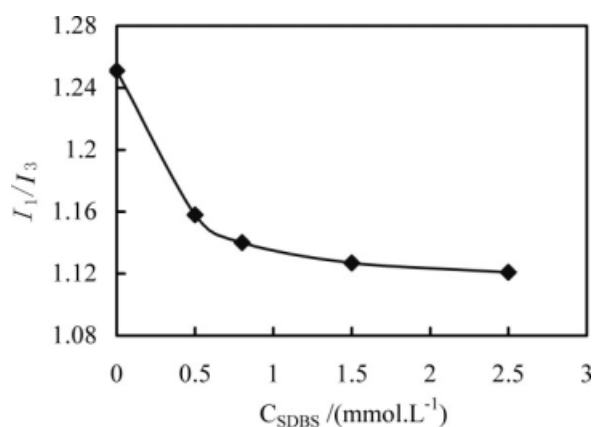


**Figure 11** Influence of the SDBS concentration ( $C_{\text{SDBS}}$ ) on the  $I_1/I_3$  values in unsalted PAAP solutions. The polymer concentration was 0.4 g/dL.

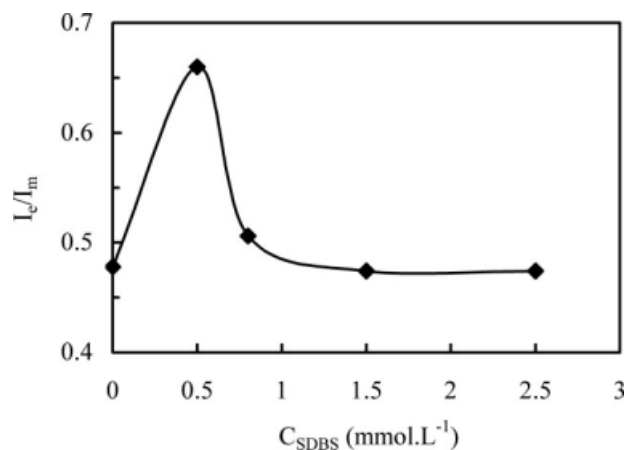


**Figure 12** Influence of the SDBS concentration ( $C_{\text{SDBS}}$ ) on the  $I_e/I_m$  values in unsalted PAAP solutions. The polymer concentration was 0.4 g/dL.

aggregates became compact because of the electrostatic shielding of intermolecular repulsions, and it was difficult for water molecules to enter hydrophobic microdomains; this led to a great increase in the solubility of pyrene in the microdomains. However, the solution viscosity decreased because of the formation of compact aggregates with small hydrodynamics volume in the PAAP brine solution.<sup>29</sup>

#### Effect of the surfactant on the aggregation of PAAP in the unsalted solutions

Figure 10 shows the pyrene emission spectra of 0.4-g/dL unsalted PAAP solutions with different sodium dodecyl benzene sulfonate (SDBS) concentrations. Figures 11 and 12 show  $I_1/I_3$  and  $I_e/I_m$  as a function of SDBS concentration, respectively. As shown in Figure 11, with the addition of 0.5-mmol/L SDBS to the polymer solution, the  $I_1/I_3$  value

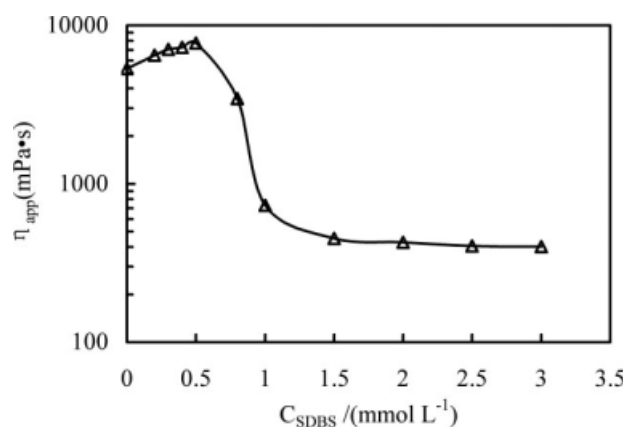


**Figure 13** Effect of the SDBS concentration ( $C_{\text{SDBS}}$ ) on the apparent viscosity ( $\eta_{\text{app}}$ ) of unsalted PAAP solutions. The polymer concentration was 0.4 g/dL.

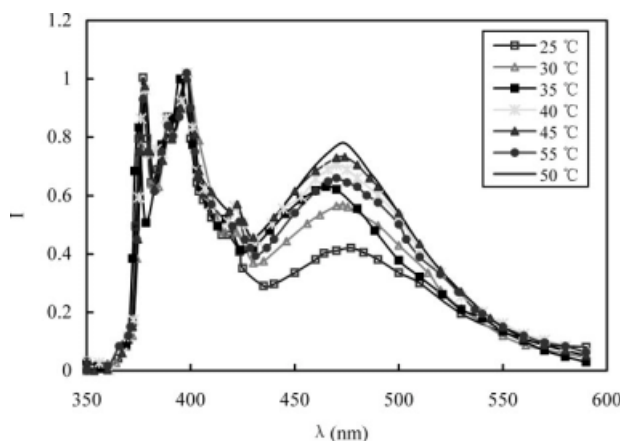


**Figure 14** Fluorescence spectra of pyrene in unsalted PAAP solutions at different temperatures ( $\lambda$  = wavelength;  $I$  = intensity). The polymer concentration was 0.5 g/dL.

sharply decreased; this indicated that the nonpolarity in the hydrophobic microdomains remarkably increased, and larger associating network structures were formed via the bridging of a small amount of surfactant molecules with hydrophobic groups. Then, the nonpolarity slightly varied above 0.5 mmol/L SDBS. The maximum of  $I_e/I_m$  also appeared at 0.5-mmol/L SDBS in Figure 12, which suggested that the degree of hydrophobic associations were the strongest, and the volumes of hydrophobic microdomains were also the largest, which resulted in the highest concentrations of pyrene excimers dissolved in the microdomains. With further increasing SDBS concentration, the  $I_e/I_m$  value sharply decreased, and then, it was almost invariable. The proposed interpretation supported by the experimental results was as follows: with increasing the surfactant concentration above 0.5 mmol/L SDBS, the number of surfactant micelles increased; the number of mixed micelles containing surfactant molecules and hydrophobic groups from different polymer chains also increased, but the number of hydrophobic groups in each mixed micelle decreased, which led to smaller sizes of microdomains. The intermolecular hydrophobic associating structures were gradually disrupted by the addition of excessive SDBS, and micellelike aggregates with individual hydrophobic segments were finally

**TABLE III**  
Influence of the Temperature on the  $I_1/I_3$  Values in the Unsalted PAAP Solutions

	Temperature (°C)						
	25	30	35	40	45	50	55
$I_1/I_3$	1.155	1.161	1.077	1.103	1.121	1.104	1.107

The polymer concentration was 0.5 g/dL.

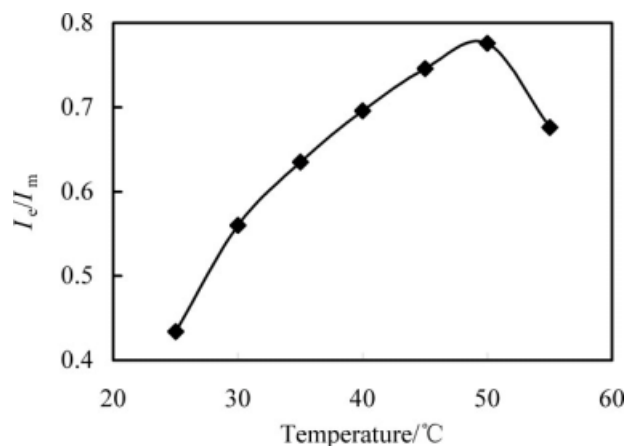


**Figure 15** Influence of temperature on the  $I_e/I_m$  values in unsalted PAAP solutions. The polymer concentration was 0.5 g/dL.

formed. The dependence of apparent viscosity on SDBS concentration (Fig. 13) further substantiated these results, and the solution viscosity dramatically increased with the addition of 0.5-mmol/L SDBS.

#### Effect of the temperature on the aggregation of PAAP in unsalted solutions

The aforementioned pyrene emission spectra were measured at 35°C. Figure 14 displays the pyrene emission spectra of 0.5-g/dL unsalted PAAP solution at different temperatures. Table III and Figure 15 show  $I_1/I_3$  and  $I_e/I_m$  as a function of temperature, respectively. With increasing temperature from 25 to 50°C, as displayed in Table I, the  $I_1/I_3$  value varied slightly. However, as shown in Figure 15, the  $I_e/I_m$  value obviously increased, and the maximum was reached at 50°C. The results imply that with increasing temperature, the variation in the nonpolarity of

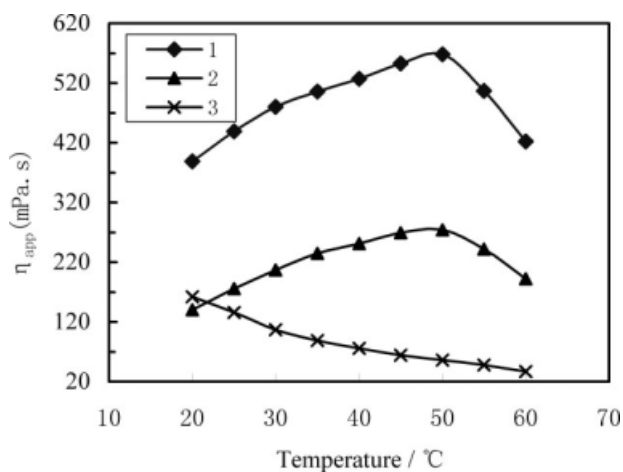


**Figure 16** Apparent viscosity ( $\eta_{app}$ ) of PAAP solutions as a function of temperature: (1) unsalted PAAP solution (0.1 g/dL), (2) 0.0855 mol/L NaCl solution of PAAP (0.2 g/dL), and (3) PAA solution (0.2 g/dL).



the microdomains was not obvious, and just the sizes and number of aggregates increased; this resulted in an increase in the concentration of pyrene excimer dissolved in the microdomains. With increasing temperature from 50 to 55°C, a small amount of hydrophobic associating structures collapsed because of faster movement of the water molecules and polymer chains, which brought about decreases in the size and number of aggregates. The variation of  $I_e/I_m$  with temperature was consistent with a plot of solution viscosity versus temperature (Fig. 16) for the unsalted PAAP solution, and the solution viscosity simply decreased with increasing temperature for the PAA polymer. Figures 15 and 16, which reflect the solution microstructure and macroscopic solution properties, respectively, demonstrate the explanation that the hydrophobic association was an endothermic process of entropy increase in a certain temperature range.<sup>30</sup>

### CONCLUSIONS

A water-soluble AM-based terpolymer (PAAP) with NaAMPS and VP as the hydrophobic monomer was synthesized by a micellar free-radical copolymerization technique. The fluorescent probe results show that strong intermolecular hydrophobic associations existed among the biphenyl groups, which led to the formation of three-dimensional networks and a high apparent viscosity for the unsalted PAAP solution, and  $C_p^*$  was 0.05 g/dL for the unsalted and brine PAAP solutions. The nonpolarity in the hydrophobic microenvironments was almost the same as that of micelles in the 0.05-mol/L SDS aqueous solution at 0.5-g/dL PAAP. With the addition of 0.256-mol/L NaCl, the  $I_1/I_3$  value decreased, and the  $I_e/I_m$  value remarkably increased; this indicated that the hydrophobic microstructures became more compact. Above 0.15-g/dL PAAP in brine solution, with increasing polymer concentration, the  $I_1/I_3$  value tended to be constant and was 1.064, but the  $I_e/I_m$  value increased throughout. With the addition of 0.5-mmol/L SDBS in the unsalted PAAP solution, the nonpolarity in the hydrophobic microdomains sharply increased, and the degree of hydrophobic association and the sizes of microdomains were maximum. At higher SDBS concentrations, the nonpolarity and microviscosity in the microenvironment were slightly invariable. With increasing temperature, the sizes and number of aggregates increased

up to 50°C, and the nonpolarity in the hydrophobic microdomains varied slightly. For influence factors including polymer concentration, surfactant, and temperature in the unsalted PAAP solutions, the microcosmic hydrophobic associations studied by the fluorescent probe were in accord with the thickening properties.

### References

- McCormick, C. L.; Nonaka, T.; Brent Johnson, C. *Polymer* 1988, 29, 731.
- McCormick, C. L.; Kramer, M. C.; Chang, Y.; Branham, K. D.; Kathmann, E. L. *Polym Prepr* 1993, 34, 1005.
- Dragan, S.; Ghimici, L. *Polymer* 2001, 42, 2886.
- Wei, Y. P.; Cheng, F. *Carbohydr Polym* 2007, 68, 734.
- Xiong, F.; Li, J.; Wang, H. et al. *Polymer* 2006, 47, 6636.
- Qian, R.; Benoit, H.; Rempp, P. *Macromolecules*; Pergamon: New York, 1982; p 159.
- Tsitsilianis, C.; Iliopoulos, I.; Ducouret, D. *Macromolecules* 2000, 33, 2936.
- Zhong, C.; Huang, R.; Zhang, X.; Dai, H. *J Appl Polym Sci* 2007, 103, 4028.
- McCormick, C. L.; Middleton, J. C.; Cummins, D. F. *Macromolecules* 1992, 25, 1201.
- Busse, K.; Kressler, J. *Macromolecules* 2002, 35, 178.
- Ye, L.; Mao, L.; Huang, R. H. *J Appl Polym Sci* 2001, 82, 3552.
- Ma, J.; Huang, R. H.; Zhao, L.; Zhang, X. *J Appl Polym Sci* 2005, 97, 316.
- Mylonas, Y.; Bokias, G.; Iliopoulos, I.; Staikos, G. *Eur Polym J* 2006, 42, 849.
- Uemura, Y.; McNulty, J.; Macdonald, P. M. *Macromolecules* 1995, 28, 4150.
- Widad, H.; Michel, D.; Michel, S.; Didier, L.; Luc, P.; Veronique, R. *J Colloid Interface Sci* 2005, 281, 316.
- Gao, B. J.; Jiang, L. D.; Kong, D. L. *Colloid Polym Sci* 2007, 285, 839.
- Talwar, S.; Scanu, L. F.; Khan, S. A. *J Rheol* 2006, 50, 831.
- Huang, Z. Y.; Lu, H. S.; He, Y. *Colloid Polym Sci* 2006, 285, 365.
- Bokias, G. *Polymer* 2001, 42, 3657.
- English, R. J.; Laurer, J. H.; Spontak, R. J.; Khan, S. A. *Ind Eng Chem Res* 2002, 41, 6425.
- Hill, A.; Candau, F.; Selb, J. *Macromolecules* 1993, 26, 4521.
- Ma, J.; Cui, P.; Zhao, L.; Huang, R. H. *Eur Polym J* 2002, 38, 1627.
- Wilhelm, M.; Zhao, C. L.; Wang, Y. *Macromolecules* 1991, 24, 1033.
- Chen, J.; Jiang, M.; Zhang, Y.; Zhou, H. *Macromolecules* 1999, 32, 4861.
- Dowling, K. C.; Thomas, J. K. *Macromolecules* 1990, 23, 1059.
- Bromberg, L. E.; Barr, D. P. *Macromolecules* 1999, 32, 3649.
- Zhong, C. R. Doctoral dissertation, Sichuan University, 2004.
- Winnik, F. M. *Chem Rev* 1993, 93.
- Zhong, C. R.; Luo, P. Y.; Meng, X. H. *J Solution Chem* 2009, 38, 485.
- Zhong, C.; Luo, P. *J Polym Sci Part B: Polym Phys* 2007, 45, 826.